A cis -Proline to Alanine Mutant of E. coli Aspartate Transcarbamoylase: Kinetic Studies and Three-Dimensional Crystal Structures † , ‡

ARTICLE *in* BIOCHEMISTRY · AUGUST 2000

Impact Factor: 3.02 · DOI: 10.1021/bi000418+ · Source: PubMed

A *cis*-Proline to Alanine Mutant of *E. coli* Aspartate Transcarbamoylase: Kinetic Studies and Three-Dimensional Crystal Structures[†,‡]

Lei Jin,[§] Boguslaw Stec,[⊥] and Evan R. Kantrowitz*[,||]

Department of Chemistry, Boston College, Merkert Chemistry Center, Chestnut Hill, Massachusetts 02467

Received February 23, 2000; Revised Manuscript Received May 5, 2000

ABSTRACT: The only *cis*-proline residue in *Escherichia coli* aspartate transcarbamoylase has been replaced by alanine using site-specific mutagenesis. The Pro268→Ala enzyme exhibits a 40-fold reduction in enzyme activity and decreased substrate affinity toward carbamoyl phosphate and aspartate compared to the corresponding values for the wild-type enzyme. The concentration of the bisubstrate analogue *N*-phosphonacetyl-L-aspartate (PALA) required to activate the mutant enzyme to the same extent as the wild-type enzyme is significantly increased. The heterotropic effects of ATP and CTP upon the Pro268→Ala enzyme are also altered. Crystal structures of the Pro268→Ala enzyme in both T- and R-states show that the *cis*-peptidyl linkage between Leu267 and Ala268 is maintained. However, the tertiary structure of both the catalytic and regulatory chains has been altered by the amino acid substitution, and the mobility of the active-site residues is increased for the R-state structure of Pro268→Ala enzyme as comparison with the wild-type R-state structure. These structural changes are responsible for the loss of enzyme activity. Thus, Pro268 is required for the proper positioning of catalytically critical residues in the active site and is important for the formation of the high-activity high-affinity R-state of *E. coli* aspartate transcarbamoylase.

The peptide bond (C−N) in proteins is rigid and planar. The hydrogen of the amino group is nearly always located opposite to the oxygen of the carbonyl group, in the trans configuration (*1*), whereas the cis configuration of peptide bonds rarely occurs in proteins due to the steric conflicts with adjacent amino acid residues (*2*, *3*). In the survey of structures deposited in the Protein Data Bank, 0.05% of the amide (X-non Pro) bonds are cis, while the occurrence of cis imide (X-Pro) peptide bonds is more frequent, at 6.5% (*2*). Proline is unique among the amino acids with its five-membered ring. Comparing the spatial conformation of cis and trans bonds, the atoms of the proline residue adjacent to the α-carbon of the preceding residue are quite similar in either configuration. In addition, the energy barrier for the trans to cis isomerization is about 13 kcal/mol for imide bonds, significantly lower than about 20 kcal/mol for amide bonds (*4*). Structurally, proline in the cis conformation allows unusual main-chain conformations, usually forming the classic type VIa and VIb turns as described by Lewis et al. (*5*). However, the functional significance of proline in the cis conformation is unclear.

Aspartate transcarbamoylase from *Escherichia coli* (EC 2.1.3.2) is an allosteric enzyme which catalyzes the committed step in the biosynthesis of pyrimidines. It catalyzes the transcarbamoylation reaction between L-aspartate and carbamoyl phosphate to form *N*-carbamoyl-L-aspartate and inorganic phosphate (*6*, *7*). The *E. coli* enzyme exhibits a sigmoidal saturation curve for aspartate indicating cooperative aspartate binding. The enzyme is also heterotropically regulated. CTP, the end-product of the pyrimidine pathway, inhibits the enzyme; UTP inhibits the enzyme synergistically in the presence of CTP; while ATP, the end-product of the parallel purine pathway, activates the enzyme (*8*−*10*).

The *E. coli* holoenzyme (M_r 310 000) is a dodecamer, composed of two catalytic trimers (M_r 33 000 for each chain) and three regulatory dimers (M_r 17 000 for each chain). The catalytic chain is composed of two structural domains, the aspartate domain (Asp) and the carbamoyl phosphate domain (CP),[1] which are involved in the binding of aspartate and carbamoyl phosphate, respectively. The regulatory chain is also composed of two domains, the allosteric (Al) and the zinc domains, which are involved in the binding of the allosteric effectors and zinc, respectively (see Figure 1).

The enzyme exists in at least two structural and functional states. In the absence of substrates, the enzyme exists in a

[†] This work was supported by National Institutes of Health (GM26237).

[‡] X-ray coordinates have been deposited in the Protein Data Bank (1EZZ and 1F1B).

* To whom correspondence should be addressed. E-mail: evan.kantrowitz@bc.edu.

[§] Present address: Lilly Research Laboratories, Eli Lilly and Company, Drop Code 0403, Indianapolis, IN 46285. Tel. (317) 433-3739; FAX (317) 276-9722; email: jin_lei @lilly.com.

[||] Boston College. Tel: (617) 552-4558. Fax: (617) 552-2705. E-mail: evan.kantrowitz@bc.edu.

[⊥] Present address: Department of Biochemistry and Cell Biology, Rice University, 6100 Main St., Houston, TX 77005. Tel. (713) 348-3346; FAX (713) 348-5154; email: stec@bioc.rice.edu.

[1] Abbreviations: PALA, *N*-phosphonacetyl-L-aspartate; CP, carbamoyl phosphate; Al, allosteric; RMS, root-mean-square; PDB, Protein Data Bank; 1D09, the R-state structure of aspartate transcarbamoylase with PALA bound deposited in the Protein Data Bank determined to 2.1 Å resolution; 6AT1, the T-state structure of aspartate transcarbamoylase deposited in the Protein Data Bank determined to 2.6 Å resolution; P268A_R, the R-state structure of the Pro268→Ala aspartate transcarbamoylase with PALA bound; P268A_T, the T-state structure of the Pro268→Ala aspartate transcarbamoylase.

10.1021/bi000418+ CCC: $19.00
Published on Web 06/16/2000

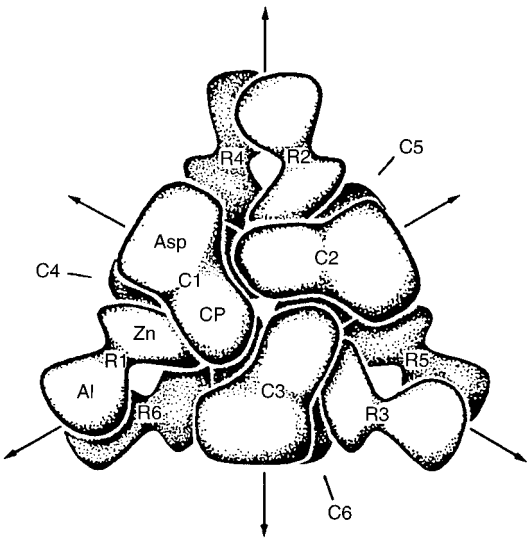

FIGURE 1: Schematic representation of the quaternary structure of aspartate transcarbamoylase viewed down the 3-fold axis (*55*). The six catalytic (C) and regulatory (R) chains are numbered. Catalytic chains C1−C2−C3 and C4−C5−C6 correspond to the two catalytic subunits, while the regulatory chains R1−R6, R2−R5, and R3−R6 correspond to the three regulatory subunits. Each catalytic chain is composed of an aspartate (Asp) and a carbamoyl phosphate (CP) domain. Each regulatory chain is composed of an allosteric (Al) and a zinc (Zn) domain.

low-activity low-affinity state (T-state), which is converted into a high-activity high-affinity enzyme (R-state) upon the binding of substrates or certain substrate analogues. The structural and functional properties of aspartate transcarbamoylase have been reviewed in detail (*11*−*15*).

E. coli aspartate transcarbamoylase has one cis-peptide bond in each of the catalytic chains, between Leu267 and Pro268. Besides the *E. coli* enzyme, the crystal structure of *B. subtilis* enzyme has also been solved (*16*). However, because of the low resolution of the structure (3.0 Å), only the positions of the α-carbon atoms were deposited in the Protein Data Bank (code 2AT2), and therefore, the conformation of the equivalent proline residue is unknown. This proline residue is not only conserved in all the known aspartate transcarbamoylases but also in the partially homologous enzyme ornithine transcarbamoylase. Both enzymes catalyze a similar transcarbamoylation reaction and have high sequence homology (*17*, *18*). In the ornithine transcarbamoylases, the equivalent proline is located in an absolutely conserved HCLP sequence motif (*19*), and is in the cis conformation in all known crystal structures of these enzymes (*20*−*23*) (with PDB code 1ORT, 1AKM, 1A1S, and 1OTH, respectively).

The *cis*-proline, residue 268, in *E. coli* aspartate transcarbamoylase is located at the active site. The carbonyl oxygen of the preceding residue, Leu267, interacts with the nitrogen of the bisubstrate analogue *N*-phosphonacetyl-L-aspartate (PALA) (*24*−*26*) bound in the active site, and several active-site residues interact with the ring of the *cis*-proline. The equivalent *cis*-proline residue is located in a similar environment in the crystal structures of *E. coli* (*27*) and human ornithine transcarbamoylase (*23*) liganded with its bisubstrate analogue *N*-phosphonacetyl-L-ornithine.

In this work, Pro268 of *E. coli* aspartate transcarbamoylase has been replaced by alanine using site-specific mutagenesis to investigate the functional role of this *cis*-proline residue. Alanine was chosen because it has the smallest side chain among the chiral amino acids. Replacement of other *cis*-proline residues has produced either a *cis*-nonproline peptide bond (*28*, *29*) or isomerization to a trans conformer with changes in the local backbone conformation (*30*). The only crystal structure of a *cis*-proline to alanine mutant reported is for human carbonic anhydrase II (*28*). The *cis*-peptidyl linkage was retained in the *cis*-Pro202→Ala mutant of carbonic anhydrase and the CO_2 hydrase activity and affinity for sulfonamide inhibitors were virtually identical to those of the wild-type enzyme.

Here we report a kinetic characterization of the Pro268→Ala mutant of *E. coli* aspartate transcarbamoylase as well as crystal structures of the mutant enzyme in the unligated T-state and in the PALA ligated R-state.

EXPERIMENTAL PROCEDURES

Materials. Agar, ampicillin, ATP, CTP, carbamoyl phosphate, *N*-carbamoyl-L-aspartate, 2-mercaptoethanol, poly(ethylene glycol) 1450, potassium dihydrogen phosphate, and uracil were obtained from Sigma Chemical Co. Q-Sepharose Fast Flow resin, ampicillin, Tris, restriction endonucleases, Thermo Sequenase radiolabeled terminator cycle sequencing kit, and T4 DNA ligase were obtained from Amersham Pharmacia Biotech. QIAprep Spin Plasmid kit was purchased from Qiagen, Inc., and Geneclean Spin kit was purchased from BIO 101 Inc. Sodium dodecyl sulfate was purchased from Bio-Rad Laboratories. Carbamoyl phosphate dilithium salt, obtained from Sigma, was purified before use by precipitation from 50% (v/v) ethanol and was stored desiccated at −20 °C (*8*). Casamino acids, yeast extract, and tryptone were obtained from Difco. Enzyme-grade ammonium sulfate and electrophoresis-grade acrylamide were purchased from ICN Biomedicals. Antipyrine was obtained from Kodak. The DNA oligomer used for the mutagenesis was purchased from Operon Technologies, Inc.

Site-Specific Mutagenesis. The Pro268 to alanine mutant of *E. coli* aspartate transcarbamoylase was constructed by introducing specific base changes in the *pyrB* gene using the Kunkel method (*31*, *32*). The uracil-containing single-stranded DNA required was obtained by infection of *E. coli* strain CJ236 containing the phagemid pEK152 (*33*) with the helper phage M13K07 (*34*). Selection of the mutations was performed directly by double-strand dideoxy sequencing (*35*).

Recloning and Confirmation of the Mutations. After the mutation was verified, a DNA fragment containing the mutation was removed with the restriction enzymes *Bst*EII and *Bgl*II and inserted into the plasmid pEK54 (*36*) that had the corresponding section of the wild-type gene removed. Following construction of the plasmid (pEK412 for Pro268→Ala), the region inserted into pEK154 was sequenced to verify that only the mutation at position 268 had occurred.

Purification of the Wild-Type and Pro268→Ala Enzymes. The wild-type and mutant enzymes were isolated as described by Nowlan and Kantrowitz (*37*) from *E. coli* strain EK1104 containing pEK2 (*38*) and pEK412, respectively. The purity of the enzyme was judged by SDS−PAGE (*39*) stained with Coomassie Blue.

Determination of Protein Concentration. The concentration of pure wild-type enzyme was determined by absorbance

measurements at 280 nm with an extinction coefficient of 0.59 cm^2/mg. The protein concentration of the mutant enzyme was determined by the Bio-Rad version of Bradford's dye-binding assay using the wild-type enzyme as standard (*40*).

Aspartate Transcarbamoylase Assay. The aspartate transcarbamoylase activity was measured at 25 °C by the colorimetric method in 0.05 M Tris-acetate buffer, pH 8.3 (*41*).

Crystallization. Crystals of the T-state Pro268→Ala mutant were obtained by the hanging-drop method. Single crystals were obtained by mixing 24 mg/mL of the Pro268→Ala enzyme, in a 1:1 ratio (v/v), with a solution of 14% (w/v) PEG 1450 and 20 mM Hepes, pH 7.0. The rhombohedral crystals, which took about 1 month to grow at 20 °C, were about 0.6 × 0.6 × 0.3 mm^3.

The R-state crystals were grown in dialysis buttons using an enzyme concentration of 7.5 mg/mL submerged in buffer containing 1 mM PALA, 20 mM maleic acid, and 3 mM sodium azide at pH 5.75, similar to the condition described by Ke et al. (*25*). The rodlike crystals, 1.6 × 0.6 × 0.6 mm^3 in size, formed overnight at 20 °C. The morphology of the crystals was very sensitive to pH. A difference of only 0.02 pH determined whether nicely formed single crystals or twined crystals were obtained.

Data Collection and Structure Refinement. The diffraction data were collected at room temperature at the crystallographic facility in the Chemistry Department of Boston College on two multiwire area detectors from Area Detector Systems mounted on a Rigaku RU-200 rotating anode generator operated at 50 kV and 150 mA. A DEC-Alpha 3300 computer controlled the data collection. Diffraction data were processed by software provided by Area Detector Systems (*42*).

The initial model for the T-state structure of the Pro268→Ala enzyme was derived from the coordinates of the wild-type structure of *E. coli* aspartate transcarbamoylase in space group *R*32, kindly provided to us by Drs. Nolte and Lipscomb. The initial model for the R-state structure was the structure of the *E. coli* enzyme with PALA bound determined to 2.1 Å (*26*). All of the water molecules in the initial models were removed. The refinements were carried out on Silicon Graphics Indigo II computers at Boston College using IMPLOR (PolyVision, Inc. Hopedale, MA), a Korn shell script driven program which automates the refinement steps running on XPLOR (*43*). IMPLOR works by setting the desired number of test sets (in our case four) to monitor R_{free} at all stages of the refinement. One data set was used for one particular step to avoid overfitting and the refinement step is accepted only if the R_{free} decreases and the difference between R and R_{free} does not increase. Water molecules are automatically added in IMPLOR from the difference map. New water molecule positions are derived and accepted if they are at a reasonable hydrogen-bonding distance with other atoms in the model. Water molecules with temperature factors higher than 79.9 were deleted.

After each round of refinement, the model was checked and manually corrected against the $2F_o - F_c$ and $F_o - F_c$ maps using the program O (*44*) and for stereochemical consistency with PROCHECK (*45*). Refinement was considered complete when the R_{free} could not be reduced further. The X-ray diffraction data and refinement statistics are summarized in Table 1. The final structure of the T-state Pro268→Ala enzyme has 246 water molecules with *R*-factors 18.2/24.2% (R_{work}/R_{free}), while the R-state Pro268→Ala structure has 1012 water molecules with *R*-factors 19.6/23.2% (R_{work}/R_{free}).

Table 1: Data Collection and Refinement Summary of the T-state and R-state of Pro268→Ala Enzyme

	T-state	R-state
data collection		
resolution (Å)	2.7	2.3
space group	*R*3	*P*321
unit cell (Å)	$a = b = 129.87$ $c = 198.34$	$a = b = 122.11$ $c = 156.21$
R_{merge}[a] (%)	7.3	6.8
completeness (%)	99.9	97.8
unique reflections	34 422	58 790
redundancy	3.2	4.4
refinement		
resolution (Å)	8−2.7	8−2.3
sigma cutoff (σ)	2	2
reflections	29 421	57 236
non-hydrogen protein atoms	7230	7230
water molecules	246	1012
average *B* (main chain/side chain, $Å^2$)		
A chain	22.5/25.7	26.4/28.5
B chain	44.6/46.9	48.3/51.2
C chain	22.5/26.2	20.7/23.0
D chain	44.5/46.5	48.1/51.5
R-factor (%)		
R_{work}	18.2	19.6
R_{free}	24.2	23.2
RMS deviations from ideal		
bonds (Å)	0.012	0.013
angles (deg)	1.86	1.74
dihedrals (deg)	25.6	25.3
improper (deg)	1.57	1.69

[a] $R_{merge} = \Sigma_{hkl}\Sigma_i|I_{mean} - I_i|\Sigma_{hkl}\Sigma_i I_i$.

Structure Comparisons. The method for comparing the mutant structures with PDB deposited T (PDB code 6AT1) and R (PDB code 1D09) structures of aspartate transcarbamoylase has been described in detail by Jin et al. (*26*). The planar angles were calculated in QUANTA (Biosym/MSI) by using three points, namely the centers of gravity of two domains of a structure and a carefully chosen hinge.

RESULTS

Steady-State Kinetics of the Wild-Type and Pro268→Ala Enzymes. The replacement of Pro268 with alanine of the catalytic chain of aspartate transcarbamoylase results in a 40-fold reduction in the observed maximal velocity as compared to the wild-type enzyme. The aspartate concentration at half of the maximal velocity, $[Asp]_{0.5}$, is increased by 15-fold, while the carbamoyl phosphate concentration at half of the maximal velocity, $[CP]_{0.5}$, is increased by 18-fold. In addition, the aspartate cooperativity, as measured by the Hill coefficient (n_H) is reduced significantly from $n_H = 2.8$ for the wild-type to $n_H = 1.6$ for the Pro268→Ala enzyme. A complete summary of the kinetic parameters is given in Table 2.

Comparison of the PALA Effect on the Wild-Type and Pro268→Ala Enzymes. At subsaturating concentrations of aspartate and saturating concentrations of carbamoyl phosphate, low concentrations of PALA activate the enzyme. This activation is due to the PALA-induced shift of the enzyme

Table 2: Kinetic Parameters for the Wild-Type and Pro268→Ala Enzymes[a]

enzyme	maximal velocity[b] (mmol/h·mg)	$[Asp]_{0.5}$[c] (mM)	n_H	$[CP]_{0.5}$[d] (mM)
wild-type	19.6	11.6	2.8	0.2
Pro268→Ala	0.5	171.8	1.6	3.6

[a] The kinetic reactions for the wild-type and the Pro268→Ala enzymes were carried out at 25 °C in 50 mM Tris-acetate buffer, pH 8.3. For the aspartate saturation curves, carbamoyl phosphate was at a saturating concentration, 5 mM for wild-type enzyme, and 15 mM for the Pro268→Ala enzyme. For the carbamoyl phosphate curves, aspartate was at a saturating concentration, 30 mM for wild-type enzyme and 375 mM for Pro268→Ala enzyme. [b] Maximal observed specific activity is measured in units of mmole of carbamoyl aspartate formed per hour per milligram of enzyme. [c] $[Asp]_{0.5}$ is the aspartate concentration at half of the maximal observed specific activity. [d] $[CP]_{0.5}$ is the carbamoyl phosphate concentration at half of the maximal observed specific activity.

from the low-activity low-affinity T-state to the high-activity high-affinity R-state. However, at higher concentrations of PALA, the activation is reduced due to competitive binding of PALA to the active sites. The shape of the PALA saturation curve for the Pro268→Ala enzyme is very similar to that for the wild-type enzyme (data not shown), with an initial activation of the enzyme activity at low PALA concentrations followed by inhibition of the enzyme activity at high PALA concentrations. The maximal activation induced by PALA is very similar for the wild-type and the Pro268→Ala enzymes; however, the concentration of PALA necessary to maximally activate the Pro268→Ala enzyme is increased by 233-fold as comparing to that for wild-type enzyme. The increased concentration of PALA necessary to maximally activate the Pro268→Ala enzyme indicates a significantly reduced affinity for the bisubstrate analogue.

ATP and CTP Effect on the Wild-Type and Pro268→Ala Enzymes. The replacement of Pro268 by alanine of the catalytic chain also alters the response of the enzyme to the allosteric regulators, ATP and CTP (Figure 2). Although the shape of the activation or inhibition curves are very similar, ATP activates the Pro268→Ala enzyme to a lesser extent, and CTP inhibits the Pro268→Ala enzyme to a greater extent than the wild-type enzyme.

Confirmation of the Pro268→Ala Mutant at Residue 268. Figure 3 shows the $F_o - F_c$ omit map for the C1 chain of the P268A_R structure. The map was calculated with XPLOR by omitting residues 267−269. The *cis*-peptidyl linkage is maintained between Leu267 and Ala268 in the P268A_R structure even though Pro268 has been replaced by Ala. The electron density at residue 268 also confirmed that this position was mutated to alanine. Similar results were also observed in the C6 chain of the P268A_R structure and both the C1 and C6 chains of the P268A_T structure (data not shown).

Main-Chain Comparison between the Pro268→Ala and Corresponding Wild-Type Structures. The overall structure of the R-state Pro268→Ala enzyme was highly similar to that of the R-state structure of the wild-type enzyme (PDB code 1D09), both determined in space group *P*321. To compare these two structures in more detail, each of the domains in the two independently determined catalytic and regulatory chains (C1:R1 and C6:R6) were superimposed separately. Only the α-carbon coordinates were selected for

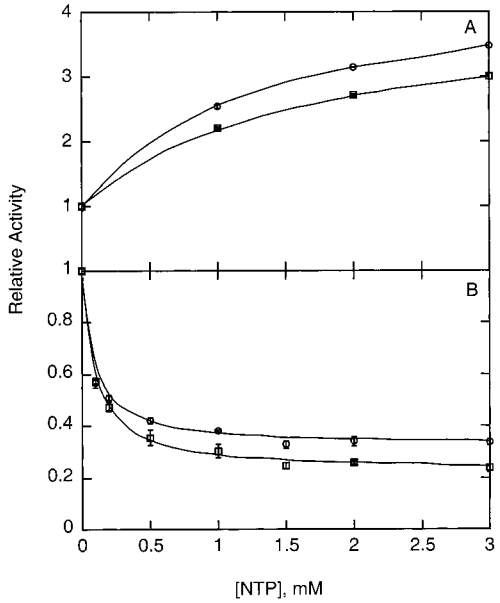

FIGURE 2: Influence of (A) ATP and (B) CTP on the activity of the wild-type (○) and Pro268→Ala (□) enzymes. Colorimetric assays were performed at 25 °C in 50 mM Tris-acetate buffer, pH 8.3 at half of the $[Asp]_{0.5}$ for the respective enzyme (6 mM for the wild-type enzyme and 85 mM for the mutant enzyme) and a saturating concentration of carbamoyl phosphate (4.8 mM for the wild-type enzyme and 15 mM for the mutant enzyme). Error bars correspond to the standard deviation.

Table 3: Individual Domain Alignments between the Pro268→Ala and Wild-Type Structures[a]

catalytic chain/state	RMS[1] Deviations(Å), α-carbons	
	CP domain	Asp domain
C1/R	0.25	0.30
C1/T	0.47	0.52
C6/R	0.21	0.23
C6/T	0.49	0.54
regulatory chain/state	**allosteric domain**	**zinc domain**
R1/R	0.59	0.32
R1/T	0.87	0.49
R6/R	0.46	0.35
R6/T	1.04	0.48

[a] The R-state structure of the Pro268→Ala enzyme is compared to the PDB file 1D09, while the T-state structure of Pro268→Ala enzyme is compared to the PDB file 6AT1. In the calculation of the RMS deviation, the following range of residues (only Cα atoms) was used: CP domain, 5−32, 37−74, 87−140, 292−305; Asp domain, 141−231, 248−269, 273−291; Allosteric domain, 15−48, 56−100; Zn domain, 101−128, 134−149. Because of their relative mobility, the N- and C-termini as well as loop regions were not included in these calculations.

comparison, with loop and turn regions excluded due to their flexible nature and the significant variations between structures. The corresponding RMS deviations are reported in Table 3. The CP domains have the least structural divergence while the allosteric domains have the most.

A similar comparison was made for the T-state Pro268→Ala structure in space group *R*3 and the wild-type structure (PDB code 6AT1) in space group *P*321. The RMS deviations between these two structures are 2-fold larger than the corresponding deviations of the R-state structures (see Table 3).

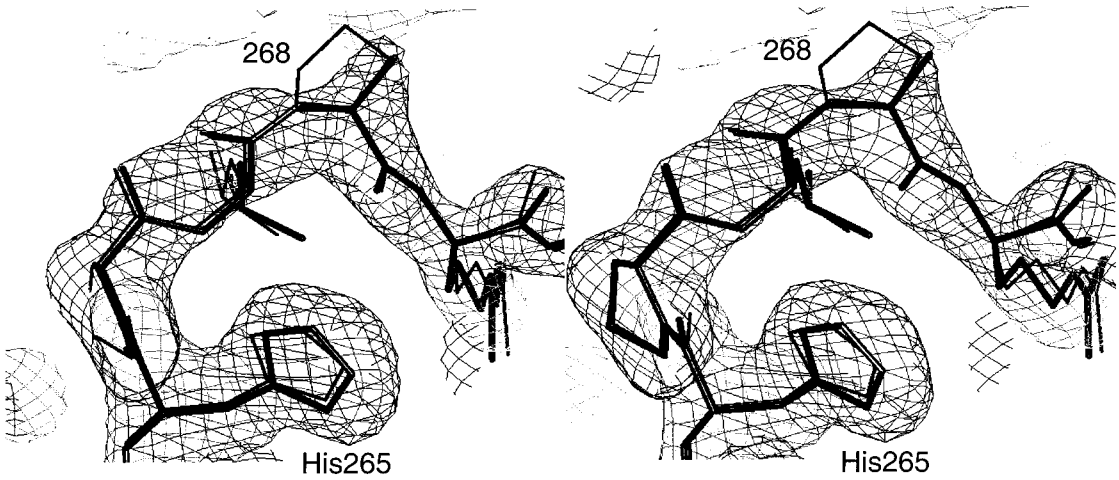

FIGURE 3: Stereodiagram of the simulated-annealing-omit electron density map in the 268 region of the P268A_R structure. Superimposed on the omit map are the structural models for the P268A_R (thick line) and wild-type (thin line) enzymes. The map was calculated from the final model with residues 267−269 omitted and contoured at 1σ. The electron density map for the P268A_R structure confirms that residue 268 was mutated to alanine. Note that the general shape of the loop in the wild-type and mutant structures is very similar.

Table 4: Planar Angle Comparison for the Structures of the Pro268→Ala and the Wild-Type Aspartate Transcarbamoylases[a]

domains in comparison[a]	planar angles between domains[a] (deg)			
	6AT1	P268A_T	1D09	P268A_R
Asp1−CP1	134.1	138.5	127.7	129.4
Asp6−CP6	135.7	137.0	128.4	125.9
CP1−Zn1	111.2	110.1	111.2	111.5
CP6−Zn6	111.3	109.8	110.8	112.2
Zn1−Al1	105.6	100.1	104.6	107.0
Zn6−Al6	105.6	101.7	103.2	103.1
Al1−Al6	153.3	152.7	155.8	155.0

[a] The number after the domain name corresponds to the particular chain in the asymmetric unit. [b] See Experimental Procedures section for definition of the planar angle.

Geometrical and Conformational Analysis for the Structures of Pro268→Ala and Wild-Type Enzymes. To compare the wild-type and mutant structures in more detail, the planar angle between domains was calculated (*26*). The planar angle represents the degree to which two domains are open. The planar angles between all pairs of domains have been calculated, as described in the Experimental Procedures, and are presented in Table 4. The angles between the CP and Asp domains for both the R-state structures (P268A_R and 1D09) are smaller than the corresponding angles in the T-state structures (P268A_T and 6AT1). The angles between CP and Asp domains are greater in the P268A_T structure than in the 6AT1 structure for both the C1 and C6 chains. In the R-state structures, the angles between CP and Asp domains for C1 and C6 are less symmetric in the P268A_R structure than in the wild-type 1D09 structure. The angles between the CP and Zn domains are highly similar in all structures. The angle between the CP and Zn domains is more open in C1:R1 than in C6:R6 in 6AT1, but less open in P268A_T. The angles between the Zn and Al domains are also different for the mutant and wild-type structures. These domains are less open in the P268A_T structure than in the 6AT1 structure, while the P268A_R structure exhibits a larger opening in the R1 chain and a similar opening in the R6 chain when compared to the 1D09 structure. The angles between the two Al domains are slightly smaller in the two mutant structures than in the corresponding wild-type structures (see Table 4).

PALA-Binding Site in P268A_R and 1D09 Structures. The active sites of aspartate transcarbamoylase are located at the cleft between CP and Asp domains at the interface with an adjacent catalytic chain. Residues that interact with PALA include Thr53, Arg54, Thr55, Arg105, His134, Arg167, Arg229, Gln231, and Leu267 along with Ser80 and Lys84 from the adjacent catalytic chain. The mutation of Pro268 to alanine changed the tertiary structure of the enzyme−inhibitor complex. In the P268A_R structure, the PALA molecule moved further away from the helix that contains residues 52−55 and closer to the loop containing Leu267. These changes are shown in Figure 4, when the atoms of the PALA molecule were aligned. There was also a shift and rotation of the active site residues in P268A_R compared with those in 1D09.

Environment Around Residue 268. As shown in Figure 4, the location of Pro268 is critical for catalysis. Pro268 is next to Leu267, an active-site residue that interacts with the nitrogen atom of PALA through its carbonyl group. The guanidino group of Arg54 interacts with the side chain of Glu86 from an adjacent chain. The side chains of both residues pack against one side of the ring of Pro268, while the side chain of Arg229 is located on the other side. The side chain of Lys84 from an adjacent chain is parallel to the ring of Pro268 against the side of the ring. Arg229 interacts with both Pro268 and Lys84. Ser80 is on the other side of Lys84 relative to Arg229, not far from Pro268. Shown in Table 5 is a comparison of the distances of these intricately related residues in the P268A_R and 1D09 structures. When Pro268 is mutated to alanine, many of these interactions are lost due to the elimination of the ring, and the distances between different atoms around residue 268 also change.

B-Factors Comparison for P268A_R and 1D09. B-Factors reflect the mobility of atoms, atoms with higher *B*-factors have higher mobility than those with lower *B*-factors. Table 6 lists the average *B*-factors for main-chain and side-chain atoms for each chain in the P268A_R and 1D09 structures. As expected the main-chain atoms have lower *B*-factors than the side-chain atoms. The average *B*-factors of the atoms of

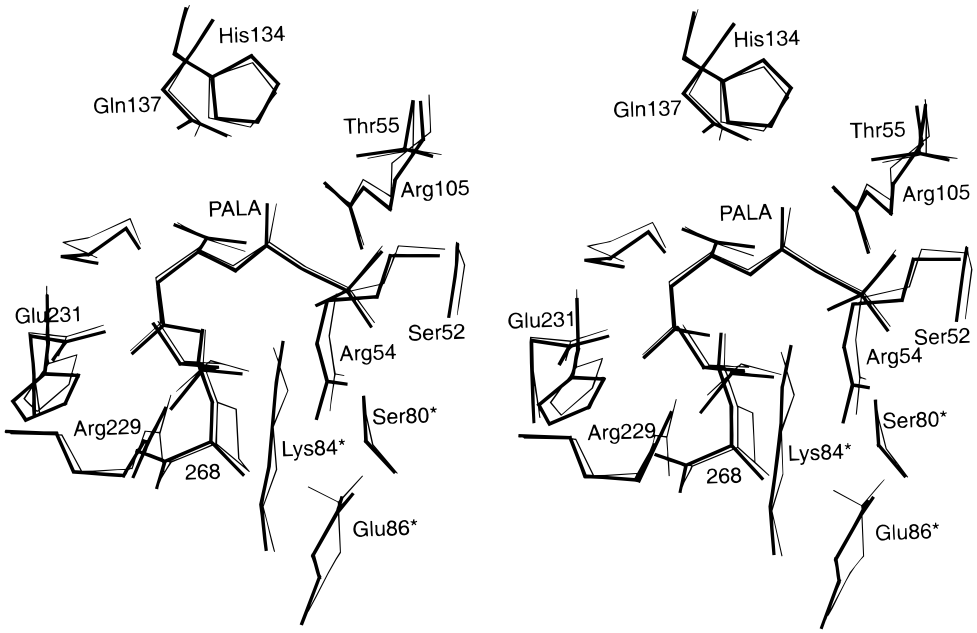

FIGURE 4: Superposition of the C1 chain active-site between the P268A_R (thick line) and the wild-type enzymes (thin line) in the R-state with PALA bound. Residues labeled with an asterisk (*) come from an adjacent catalytic chain. For the figure, the PALA molecules in the two structures were superimposed. Although the general shape of the loop containing residue 268 did not change, the relative positions of some of the active-site residues that interact with PALA are shifted and rotated a little between the two structures.

Table 5: Comparison of Distances for Residues Surround Residue 268 in the P268A_R and 1D09 Structures

		C1 distance (Å)		C6 distance (Å)	
atom	atom	1D09	P268A_R	1D09	P268A_R
268_N	Arg54_CZ	4.41	4.70	4.04	3.96
268_CB	Arg229_CD	5.11	4.89	4.62	5.06
Pro268_CG	Arg229_CD	3.95		4.52	
268_CB	Lys84_CB	4.50	4.50	4.43	4.37
Pro268_CG	Lys84_CD	3.71		3.60	
Pro268_CD	Lys84_CD	3.81		3.91	
268_CB	Ser80_CB	4.44	4.48	4.68	4.65
Pro268_CG	Ser80_CB	4.09		3.73	
268_CB	Glu86_CD	3.34	3.57	3.78	3.20
Pro268_CD	PALA_C5	4.17		3.93	
Arg229_CZ	Lys84_CD	3.54	3.87	3.57	3.67
Ser80_CB	Lys84_CD	3.98	3.74	4.21	3.99
Lys84_NZ	PALA_N1	4.03	3.84	4.08	4.09

Table 6: Comparison of the *B*-Factors for the P268A_R and Wild-Type R-State Structures

chain name	P268A_R	1D09
average *B*-factors of the atoms for each chain (Å^2) (main chain/side chain)		
C1	26.35/28.49	25.07/28.46
C6	20.71/23.05	20.22/23.82
R1	48.19/51.29	52.56/59.38
R6	47.99/51.56	54.26/59.65
overall	31.65/34.36	32.81/37.29
all protein atoms	32.97	35.00
average *B*-factors for the residues at the active site[a] (Å^2) (main chain/side chain)		
C1	19.27/18.11	14.57/11.63
C6	17.03/14.79	11.93/10.10
overall	18.19/16.51	13.30/10.90
all atoms	17.29	12.00

[a] The residues at the active site included Ser52−Thr55, Ser80, Lys84, Arg105, His134, Arg167, Arg229, Gln231, and Pro266−Arg269.

the catalytic chains in the two structures are very similar while the average *B*-factors of the atoms are lower in the P268A_R structure for the regulatory chains. The average *B*-factor for all atoms of the P268A_R structure is 32.97 Å^2, slightly lower than 35.00 Å^2 for the 1D09 structure. Also shown in Table 6 is a comparison of the *B*-factors for the residues in the active site including Ser52−Thr55, Ser80, Lys84, Arg105, His134, Arg167, Arg229, Gln231, and Pro266−Arg269. For these residues, the *B*-factors for the main-chain atoms are higher than the side-chain atoms. The average *B*-factors for the chosen atoms of the P268A_R structure are 5 Å^2 higher than that of the 1D09 structure.

DISCUSSION

The occurrence of a *cis*-peptidyl linkage is rather uncommon in proteins (*2*). However, in all known crystal structures of both aspartate and ornithine transcarbamoylases, the conserved residue Pro268 exists in the cis conformation. As seen in Figure 4, Pro268 is located close to the active site, and therefore, it was of interest to determine if the cis configuration of this amino acid is important for either structural stabilization or the function of aspartate transcarbamoylase.

When Pro268 is mutated to alanine, the functional properties of the enzyme are dramatically altered. Catalytic activity decreases 40-fold, and the affinity of the enzyme for both of its substrates as well as the bisubstrate analogue PALA is decreased substantially (see Table 2). Homotropic cooperativity is reduced but not eliminated as verified by the ability of inhibitor PALA to activate the mutant enzyme to the same extent as the wild-type enzyme. These results indicate that the alanine substitution at position 268 does not hinder the ability of the mutant enzyme to undergo the allosteric transition from the T to the R-state; however, the Pro268→Ala enzyme requires a 233-fold higher concentration of PALA to achieve maximal activation, indicating the mutation has induced a significant loss of affinity for this analogue. The dramatic decrease in catalytic activity as well

as the affinity of the enzyme for its substrates suggests that the replacement of Pro268 by alanine is causing structural alterations.

To determine if the replacement of Pro268 by alanine causes alterations to either the tertiary or quaternary structure of aspartate transcarbamoylase, the three-dimensional structure of the Pro268→Ala enzyme was determined in the absence and presence of PALA. As seen in Figure 3, the *cis*-peptidyl linkage is still preserved between Leu267 and Ala268. The conformation of the loop containing the *cis*-peptidyl linkage is essentially the same in both the mutant and wild-type structures (Figure 4). The retention of the conformation of this loop suggests that the intra- and intermolecular interactions around residue 268 play an important role in stabilizing the cis conformation.

The strategically important location of cis Pro268 within the active-site area suggests that even subtle alterations in the local environment of this region may dramatically influence the function of the enzyme. The cis conformation at this location is a necessary requirement to orient the loop in this region so that the main-chain nitrogen atom of Leu267 is directed toward the active site for the binding of substrates. Pro268 also maintains the integrity of the active site by interacting with Arg229, Arg54 of the same chain and Lys84, Ser80, and Glu86 of the adjacent chain (Figure 4). As has been determined by site-specific mutagenesis experiments, these active-site residues are essential for substrate binding and/or enzyme activity. Arg229 interacts with the substrate aspartate and also stabilizes Lys84 from a neighboring catalytic chain. Substitution of Arg229 by Ala decreases enzyme activity by 10 000-fold and the affinity for aspartate by 2-fold (*46*). When Arg54 was replaced by alanine, the resulting mutant enzyme exhibited an approximately 17 000-fold reduction in enzyme activity with little change in substrate affinity (*47*).

Mutation of Pro268 to alanine does not alter the general conformation of the loop containing residue 268. However, the loss of the interactions between the ring of Pro268 and residues within the active site results in a decrease in the stability of these residues in the R-state mutant structure as compared to the wild-type structure (see Table 5). This is reflected by the 5 Å^2 increase in the average *B*-factors for the atoms of the active-site residues in the mutant structure when compared to the average *B*-factors for the atoms of the active-site residues in the 1D09 structure (Table 6). A similar decrease in stability was reported for the Pro202 to alanine mutant of carbonic anhydrase II (*28*), although the mutation did not alter the hydrase activity of the enzyme. Increasing the mobility of the active-site residues in the Pro268→Ala mutant may be one factor for the observed decrease in substrate affinity and enzyme activity. Thus, proline at residue 268 is most likely required for properly positioning the active-site residues to achieve high activity and high substrate affinity.

The replacement of Pro268 by alanine may also alter the ability of Lys84 to function in catalysis. Upon the basis of the 1D09 structure, Jin et al. (*26*) modeled the transition state into the R-state structure of the enzyme. This transition-state model suggests that the ϵ-amino group of Lys84 acts as a base to accept the proton from the amino group of aspartate as the tetrahedral intermediate is formed (*26*). The change in the character of the peptide bond due to the Pro268 to Ala substitution results in a charge redistribution, which would result in an alteration in the polarity of the carbonyl oxygen. This oxygen was found to be important for binding and polarization of the tetrahedral transition state (*26*). Furthermore, the closeness of the ϵ-amino group of Lys84 to the cis peptidyl bond may also influence its pK_a. Alterations to either the position or pK_a of ϵ-amino group of Lys84 would influence both catalysis, substrate, and PALA binding as is observed for the Pro268→Ala enzyme.

As has been well established, the tertiary and quaternary structural changes are crucial for the activity and regulatory properties of aspartate transcarbamoylase. The catalytic mechanism for the transcarbamoylase reaction is ordered with carbamoyl phosphate binding before aspartate and *N*-carbamoyl-L-aspartate leaving before phosphate (*48*). Evidence from small-angle X-ray solution scattering (*49*) as well as ultraviolet (*50*) and circular dichroism spectroscopy (*51*) indicates that the binding of carbamoyl phosphate induces local conformational changes priming the binding site of aspartate, while the binding of aspartate results in the large quaternary conformational change. During the quaternary conformational change, the enzyme undergoes a significant expansion along the 3-fold axis amounting to approximately 11 Å. Along with this expansion along the 3-fold axis, the upper and lower catalytic subunits rotate about the 3-fold axis and the regulatory subunits rotate about their respective 2-fold axes. In addition to these quaternary conformational changes, there are also alterations in the relative positions of the domains of both the catalytic and regulatory chains. The CP and Asp domains of the catalytic chain and Al and Zn domains of regulatory chain undergo domain closure, while the two allosteric domains of the adjacent regulatory chains undergo domain opening (see Table 4, 6AT1 and 1D09). The single point mutation at residue 268 does not alter the ability of the enzyme to undergo the structural transition from the T to the R-state. The P268A_T and P268A_R structures are overall similar to the corresponding T and R-states of the wild-type enzyme, with just relatively small alterations of individual side chains and small movements of the domains. A comparison of the T-state structures of the mutant and wild-type enzymes reveals that there are structural changes within each domain (Table 3) and in the relative positions of the domains (Table 4, 6AT1 and P268A_T). These differences may come from different crystal-packing environments arising from the different space groups of the wild-type and mutant structures. Without a T-state crystal structure in the *R*3 space group, it is impossible at this point to distinguish the different contributing sources. For the R-state structure, the differences between P268A_R and 1D09 structures are caused by the mutation, since they are crystallized under the same conditions and in the same space group. The conformation of each domain is very similar for the R-state structures of the mutant and wild-type enzymes. The RMS deviations reported in Table 3 are comparable to the values obtained when two wild-type aspartate transcarbamoylase structures with PALA bound are compared (*26*). However, the tertiary structure of the mutant enzyme has considerable changes in regard to the relative positions of the domains with respect to one another. As shown in Table 4, the angle between the CP and Asp domains is more open in C1 and less open in C6 of the mutant structure compared to the wild-type structure, while the angle

between the Al and Zn domains is more open in the R1 chain of the mutant structure. Thus, the asymmetry between C1:R1 and C6:R6 is increased by the mutation of residue 268. As stated above, the relative locations of domains are critical for the activity of the enzyme. These tertiary structure changes result in changes in the orientation and the distance between active-site residues to the PALA molecule (Figure 4), which must in turn result in the decrease of substrate affinity and enzyme activity. In the P268A_R structure, the relative positions of the residues surrounding the active site do not change significantly in comparison with the 1D09 structure (Table 5). This may be caused by the strong interaction between the enzyme and the bisubstrate analogue PALA. In both the P268A_R and 1D09 structures, the *B*-factors for the side-chain atoms of the active-site residues are lower than that for the main-chain atoms (see Table 6). This indicates that the side-chain atoms of the active-site residues are less mobile than the main-chains atoms because they are "locked" by their interactions with PALA. However, the higher *B*-factors for the atoms (all atoms) of the active-site residues in the P268A_R structure may directly reflect the weakened binding of the bisubstrate analogue.

The combination of the weaker activation by ATP and stronger inhibition by CTP may be interpreted as a stabilization of the functional R-state with significantly diminished affinity for the transition state. However, the changes in the relative positions of the domains within the quaternary organization of the mutant enzyme point out that the structural R-state of the mutant enzyme is not identical to that of the wild-type enzyme. In the R-state structure of the mutant enzyme, the angle between the allosteric domains of the regulatory chains is more closed as compared to the wild-type enzyme as well as the angle between the domains in the catalytic chains, indicating an incomplete transition to the structural R-state. All these data provide evidence that the structural changes are extensive and that a global mechanism is responsible for propagation of the heterotropic response rather than a series of localized structural changes.

In this study, we have investigated the requirement for a *cis*-peptidyl linkage in *E. coli* aspartate transcarbamoylase by site-specific mutagenesis, enzyme kinetics, and protein crystallography. Our results suggest that the *cis*-peptidyl linkage between Leu267 and Pro268 in aspartate transcarbamoylase is essential for preserving the integrity of the active site for high enzyme activity, substrate affinity, as well as for keeping the proper tertiary structure of the enzyme for heterotropic signal transmission.

REFERENCES

1. Ramachandran, G. N., and Sasisekharan, V. (1968) *Adv. Protein Chem. 23*, 283−438.
2. Stewart, D. E., Sarkar, A., and Wampler, J. E. (1990) *J. Mol. Biol. 214*, 253−260.
3. MacArthur, M. W., and Thornton, J. M. (1991) *J. Mol. Biol. 218*, 397−412.
4. Schultz, G. D., and Schirmer, R. H. (1978) *Principles of Protein Structure*, Springer-Verlag, New York.
5. Lewis, P. N., Momany, F. A., and Scheraga, H. A. (1973) *Biochim. Biophys. Acta 303*, 211−229.
6. Jones, M. E., Spector, L., and Lipmann, F. (1955) *J. Am. Chem. Soc. 77*, 819−820.
7. Reichard, P., and Hanshoff, G. (1956) *Acta Chem. Scand. 10*, 548−560.
8. Gerhart, J. C., and Pardee, A. B. (1962) *J. Biol. Chem. 237*, 891−896.
9. Gerhart, J. C., and Pardee, A. B. (1963) *Cold Spring Harbor Symp. Quantum Biol. 28*, 491−496.
10. Wild, J. R., Loughrey-Chen, S. J., and Corder, T. S. (1989) *Proc. Natl. Acad. Sci. U.S.A. 86*, 46−50.
11. Lipscomb, W. N. (1992) *Proc. Robert A. Welch Found. Conf. Chem. Res., 36th (Regulation of Proteins by Ligands)*, pp 103−143, The Robert A. Welch Foundation, Houston.
12. Lipscomb, W. N. (1994) *Adv. Enzymol. 68*, 67−151.
13. Allewell, N. M. (1989) *Annu. Rev. Biophys. Chem. 18*, 71−92.
14. Kantrowitz, E. R., and Lipscomb, W. N. (1990) *Trends Biochem. Sci. (Pers. Ed.) 15*, 53−59.
15. Kantrowitz, E. R., and Lipscomb, W. N. (1988) *Science 241*, 669−674.
16. Stevens, R. C., Reinisch, K. M., and Lipscomb, W. N. (1991) *Proc. Natl. Acad. Sci. U.S.A. 88*, 6087−6091.
17. Houghton, J. E., Bencini, D. A., O'Donovan, G. A., and Wild, J. R. (1984) *Proc. Natl. Acad. Sci. U.S.A. 81*, 4864−4868.
18. Houghton, J. E., O'Donovan, G. A., and Wild, J. R. (1989) *Nature 338*, 172−174.
19. Hatziloukas, E., and Panopoulos, N. J. (1992) *J. Bacteriol. 174*, 5895−5909.
20. Villeret, V., Tricot, C., Stalon, V., and Dideberg, O. (1995) *Proc. Natl. Acad. Sci. U.S.A. 92*, 10762−10766.
21. Jin, L., Seaton, B. A., and Head, J. F. (1997) *Nat. Struct. Biol. 4*, 622−625.
22. Villeret, V., Clantin, B., Tricot, C., Legrain, C., Roovers, M., Stalon, V., Glansdorff, N., and Van Beeumen, J. (1998) *Proc. Natl. Acad. Sci. U.S.A. 95*, 2801−2806.
23. Shi, D., Morizono, H., Ha, Y., Aoyagi, M., Tuchman, M., and Allewell, N. M. (1998) *J. Biol. Chem. 273*, 34247−34254.
24. Krause, K. L., Voltz, K. W., and Lipscomb, W. N. (1987) *J. Mol. Biol. 193*, 527−553.
25. Ke, H.-M., Lipscomb, W. N., Cho, Y., and Honzatko, R. B. (1988) *J. Mol. Biol. 204*, 725−747.
26. Jin, L., Stec, B., Lipscomb, W. N., and Kantrowitz, E. R. (1999) *Proteins: Struct., Funct., Genet. 37*, 729−742.
27. Ha, Y., McCann, M. T., Tuchman, M., and Allewell, N. M. (1997) *Proc. Natl. Acad. Sci. U.S.A. 94*, 9550−9555.
28. Tweedy, N. B., Nair, S. K., Paterno, S. A., Fierke, C. A., and Christianson, D. W. (1993) *Biochemistry 32*, 10944−10949.
29. Mayr, L. M., Willbold, D., Rosch, P., and Schmid, F. X. (1994) *J. Mol. Biol. 240*, 288−293.
30. Hodel, M. R., Kautz, R. A., Jacobs, M. D., and Fox, R. O. (1993) *Protein Sci. 2*, 838−850.
31. Kunkel, T. A. (1985) *Proc. Natl. Acad. Sci. U.S.A. 82*, 488−492.
32. Kunkel, T. A., Roberts, J. D., and Zakour, R. A. (1987) *Methods Enzymol. 154*, 367−382.
33. Baker, D. P., and Kantrowitz, E. R. (1993) *Biochemistry 32*, 10150−10158.
34. Vieira, J., and Messing, J. (1987) *Methods Enzymol. 153*, 3−11.
35. Sanger, F., Nicklen, S., and Coulson, A. R. (1977) *Proc. Natl. Acad. Sci. U.S.A. 74*, 5463−5467.
36. Xu, W., Pitts, M. A., Middleton, S. A., Kelleher, S. A., and Kantrowitz, E. R. (1988) *Biochemistry 27*, 5507−5515.
37. Nowlan, S. F., and Kantrowitz, E. R. (1985) *J. Biol. Chem. 260*, 14712−14716.
38. Smith, K. A., Nowlan, S. F., Middleton, S. A., O'Donovan, C., and Kantrowitz, E. R. (1986) *J. Mol. Biol. 189*, 227−238.
39. Laemmli, U. K. (1970) *Nature (London) 227*, 680−685.
40. Bradford, M. M. (1976) *Anal. Biochem. 72*, 248−254.
41. Pastra-Landis, S. C., Foote, J., and Kantrowitz, E. R. (1981) *Anal. Biochem. 118*, 358−363.
42. Howard, A. J., Nielsen, C., and Xuong, N. h. (1985) *Methods Enzymol. 114*, 452−471.
43. Brünger, A. T. (1992) *X-PLOR, Version 3.1, A system for crystallography and NMR*, Yale University Press, New Haven.
44. Jones, T. A., Zou, J.-Y., Cowan, S. W., and Kjeldgaard, M. (1991) *Acta Crystallogr., Sect. A47*, 110−119.

45. Laskowski, R. A., MacArthur, M. W., Moss, D. S., and Thornton, J. M. (1993) *J. Appl. Crystallogr. 26*, 283−291.
46. Middleton, S. A., Stebbins, J. W., and Kantrowitz, E. R. (1989) *Biochemistry 28*, 1617−1626.
47. Stebbins, J. W., Xu, W., and Kantrowitz, E. R. (1989) *Biochemistry 28*, 2592−2600.
48. Wedler, F. C., and Gasser, F. J. (1974) *Arch. Biochem. Biophys. 163*, 57−68.
49. Fetler, L., Tauc, P., and Vachette, P. (1997) *J. Appl. Crystallogr. 30*, 781−786.
50. Collins, K. D., and Stark, G. R. (1969) *J. Biol. Chem. 244*, 1869−1877.
51. Griffin, J. H., Rosenbusch, J. P., Weber, K. K., and Blout, E. R. (1972) *J. Biol. Chem. 247*, 6482−6490.
52. Aucoin, J. M., Pishko, E. J., Baker, D. P., and Kantrowitz, E. R. (1996) *J. Biol. Chem. 271*, 29865−29869.
53. Stebbins, J. W., Zhang, Y., and Kantrowitz, E. R. (1990) *Biochemistry 29*, 3821−3827.
54. Baker, D. P., Stebbins, J. W., DeSena, E., and Kantrowitz, E. R. (1994) *J. Biol. Chem. 269*, 24608−24614.
55. Gouaux, J. E., and Lipscomb, W. N. (1990) *Biochemistry 29*, 389−402.

BI000418+